



**HAL**  
open science

## Combination of surfactants and organic compounds for boosting CO<sub>2</sub> separation from natural gas by clathrate hydrate formation

M. Ricaurte, Christophe Dicharry, X. Renaud, Jean-Philippe Torre

► **To cite this version:**

M. Ricaurte, Christophe Dicharry, X. Renaud, Jean-Philippe Torre. Combination of surfactants and organic compounds for boosting CO<sub>2</sub> separation from natural gas by clathrate hydrate formation. *Fuel*, 2014, 122, pp.206-217. 10.1016/j.fuel.2014.01.025 . hal-01816787

**HAL Id: hal-01816787**

**<https://hal.science/hal-01816787>**

Submitted on 16 Jan 2019

**HAL** is a multi-disciplinary open access archive for the deposit and dissemination of scientific research documents, whether they are published or not. The documents may come from teaching and research institutions in France or abroad, or from public or private research centers.

L'archive ouverte pluridisciplinaire **HAL**, est destinée au dépôt et à la diffusion de documents scientifiques de niveau recherche, publiés ou non, émanant des établissements d'enseignement et de recherche français ou étrangers, des laboratoires publics ou privés.




## Open Archive Toulouse Archive Ouverte (OATAO)

OATAO is an open access repository that collects the work of Toulouse researchers and makes it freely available over the web where possible

This is an author's version published in: <http://oatao.univ-toulouse.fr/21628>

**Official URL:** <https://doi.org/10.1016/j.fuel.2014.01.025>

**To cite this version:**

Ricaurte, Marvin and Dicharry, Christophe and Renaud, Xavier and Torr , Jean-Philippe  *Combination of surfactants and organic compounds for boosting CO2 separation from natural gas by clathrate hydrate formation.* (2014) *Fuel*, 122. 206-217. ISSN 0016-2361

Any correspondence concerning this service should be sent to the repository administrator: [tech-oatao@listes-diff.inp-toulouse.fr](mailto:tech-oatao@listes-diff.inp-toulouse.fr)

# Combination of surfactants and organic compounds for boosting CO<sub>2</sub> separation from natural gas by clathrate hydrate formation

Marvin Ricaurte<sup>a</sup>, Christophe Dicharry<sup>a</sup>, Xavier Renaud<sup>b</sup>, Jean-Philippe Torr <sup>a,\*</sup>

<sup>a</sup>Univ. Pau & Pays Adour, CNRS, TOTAL – UMR 5150, LFC-R – Laboratoire des Fluides Complexes et leurs R servoirs, Avenue de l'Universit , BP 1155, PAU F-64013, France

<sup>b</sup>Total – Centre Scientifique et Technique Jean-F ger (CSTJF), Avenue Larribau, PAU F-64018, France

## H I G H L I G H T S

- Combination of surfactants and organic additives enhance hydrate-based processes.
- Action mechanism based on the successive formations of (sII) and (sI) hydrates.
- THF + SDS is the best association of additives among all the combinations tested.
- Enclathration rate and selectivity of the separation remain too low for scale-up.

## A R T I C L E I N F O

### Keywords:

Gas hydrate  
Additives  
Carbon dioxide separation  
Natural gas  
Promoters

## A B S T R A C T

This study investigates the effects of several combinations of surfactants and organic compounds on the separation of CO<sub>2</sub> from a CO<sub>2</sub>–CH<sub>4</sub> gas mixture by clathrate hydrate formation. Seven additives, three surfactants (SDS, SDBS, DATCl) and four organic compounds (THF, 1,3-dioxolane, 2-methyl-tetrahydrofuran and cyclopentane) were tested for various operating conditions and at different concentrations. The influence of these additives on the quantity of gas removed, the selectivity of the separation toward CO<sub>2</sub>, and the kinetics of hydrate formation were analyzed through experiments in a batch reactor. It was found that a suitable combination of a surfactant and an organic compound can, in some cases, strongly enhance the hydrate crystallization. The best results were obtained with a combination of the additives SDS and THF.

## 1. Introduction

Clathrate hydrates are non-stoichiometric, ice-like crystalline solids formed by a three-dimensional network of hydrogen-bonded water molecules (called host molecules), which can encage various species (called guest molecules) such as methane, carbon dioxide, cyclopentane, and acetone [1] in their cavities. These supra-molecular structures exist only when there are guest molecules in the cages, and are stable in precise thermodynamic conditions specific to the host–guest system considered. When the guest molecule is a gas, the clathrate hydrate is called a “gas hydrate”, or simply “hydrate” for short. The three main hydrate structures are “structure one”, “structure two”, and “structure H”, usually denoted (sI), (sII), and (sH), respectively. Structures (sI) and (sII) are of particular interest to the Oil and Gas industry as they can accommodate small gas molecules present in natural

gas [2]. Many other details on these structures (geometry, suitable guests, etc.) can be found elsewhere [3].

Practical applications involving hydrates have recently been proposed in sectors such as energy, transport and storage of gases, refrigeration and gas separation [4]. The use of clathrate hydrates as a gas separation technique is currently at the laboratory proof-of-concept stage. The principle of the separation is based on the following analysis: when the gas hydrate is formed from an initial gas mixture (e.g. a binary mixture A + B), the final composition of the gas enclathrated into the hydrate phase will be different from the composition of the vapor phase remaining at equilibrium with the hydrate formed. Therefore, one of the components initially present in the gas (e.g. component A) will be predominantly included in the hydrate phase. Later, the hydrates formed can still be dissociated, both to recover the enclathrated gas (in this case, a gas richer in component A) and to recycle the water. Theoretically, the process seems attractive, but in practice, several points need closer investigation before any application at industrial scale. They include the hydrate formation rate, and the quantity of the component to remove from the gas mixture (which

\* Corresponding author. Tel.: +33 (0)5 40 17 51 09; fax: +33 (0)5 79 40 77 25.

E-mail address: [jean-philippe.torre@univ-pau.fr](mailto:jean-philippe.torre@univ-pau.fr) (J.-P. Torr ).

will be enclathrated in the hydrate phase), both of which must be as high as possible. Numerous hydrate-based separations have already been studied with different gas mixtures containing carbon dioxide (CO<sub>2</sub>), methane (CH<sub>4</sub>), hydrogen sulfide (H<sub>2</sub>S), sulfur hexafluoride (SF<sub>6</sub>) and others gases [5]. This process may prove an interesting alternative to conventional separation techniques (e.g. reactive absorption using alkanolamines) [6], and economically competitive for separating greenhouse gases such as SF<sub>6</sub> [7] or CO<sub>2</sub> [8].

Natural gas is considered to be one of the major energy sources for the future due to its comparative abundance on Earth, its relatively low environmental footprint compared to petroleum, and the multiple applications possible in various sectors of the economy [9]. After extraction from the reservoir, the natural gas is transported to processing units for pre-treatment. In this raw state, the gas mixture is complex as it contains hydrocarbons – primarily alkanes (paraffins), predominantly methane – and a variety of other non-hydrocarbon species such as water, nitrogen, helium and acid gases [10]. Carbon dioxide is one of the major contaminants of natural gas, and has to be separated from the methane to reach the commercial specifications. Gas reservoirs can contain a variable proportion of CO<sub>2</sub>, ranging from a few percent up to 75 vol%. Examples of gas fields with a very high concentration of CO<sub>2</sub> are the offshore Natuna gas field in Indonesia (71% of CO<sub>2</sub>) [11] or the onshore El Trapial field in Argentina (where light oil coexists with gas containing concentrations of CO<sub>2</sub> greater than 75%) [12].

Owing to the proximity of the CO<sub>2</sub> and CH<sub>4</sub> [13–15] hydrate equilibrium curves, it is fairly difficult to efficiently separate CO<sub>2</sub> from a CO<sub>2</sub>–CH<sub>4</sub> gas mixture using a hydrate-based process. However, recent results have shown that adding certain chemicals to the water, such as surfactants, organic molecules or salts, can significantly: (i) enhance the hydrate formation rate [16,17], (ii) modify the position of the equilibrium curves [18,19] and/or (iii) allow the selective enclathration of one of the gases in the hydrate phase [20].

Among the numerous additives reported in literature tested for hydrate applications, many of them can be classified in two classes, named “kinetic additives” and “thermodynamic additives”: (i) kinetic additives, generally used at low concentration (ranging from about ten to few thousands of ppm), are not included in the hydrate cavities and enhance (kinetic promoters) – or decrease (kinetic inhibitors) – the hydrate formation rate without any effect on the equilibrium conditions; (ii) “thermodynamic additives” modify the hydrate equilibrium conditions compared to the same system without additive, due to their presence into the cages of the hydrate structure or their ability to modify the activity of water. Similarly to kinetic ones, they are either promoters or inhibitors.

Interestingly, it is apparent that: (i) several surfactants are able to enhance the hydrate formation kinetics at very low dosage (such as a few hundred of ppm in water) [21,22]; and (ii) several organic molecules, particularly those which have a 5-membered cyclic structure derived from the cyclopentane, have also been reported to act as efficient thermodynamic promoters [23,24]. However, very few works address combinations of additives. Even the two most commonly cited hydrate promoters, sodium dodecyl sulfate (SDS) – a well-known anionic surfactant – and tetrahydrofuran (THF) – a cyclic ether – have rarely been used together. The authors have recently shown that a combination of these two additives can work very well in the presence of pure carbon dioxide [25] and with a CO<sub>2</sub> + CH<sub>4</sub> gas mixture [26].

This paper presents hydrate formation studies performed using various combinations of two types of additives: kinetic and thermodynamic. The objective is to analyze the effect of these combinations on the enclathration kinetics, process capacity and

efficiency of the CO<sub>2</sub> separation from a CO<sub>2</sub>–CH<sub>4</sub> gas mixture. Three surfactants (anionic and cationic) and four organic compounds (water-soluble or not) were tested at different concentrations, in various process operating conditions.

## 2. Parameters for process performance

Five parameters were defined for this study to analyze, compare the results, and quantify the process performance:

- The *quantity of gas removed* is the total mol number of gas removed from the gas phase, the reference being the total number of gas initially loaded in the reactor. This quantity can be calculated with the following equation:

$$\text{CO}_2^r + \text{CH}_4^r = \text{CO}_2^{\text{init}} + \text{CH}_4^{\text{init}} - (\text{CO}_2^{\text{hyd}} + \text{CH}_4^{\text{hyd}} + \text{CO}_2^{\text{aq}} + \text{CH}_4^{\text{aq}}) \quad (1)$$

where superscripts *r*, *init*, *hyd* and *aq* correspond to the gas removed from the gas phase, the gas initially loaded in the reactor, the gas present in the hydrate phase(s), and the gas solubilized into the aqueous solution, respectively.

In this work, the quantity of gas removed is determined by a mass balance between the initial and final states. The molar quantities necessary for the calculations are obtained by using: (i) the gas compositions obtained by GC analyses; and (ii) the Peng–Robinson Equation of State (PR–EOS), used with classical mixing rules, to calculate the molar volume of the gas mixtures at operating conditions. For further details, the complete set of the equations can be found elsewhere [27].

- *S* is the *selectivity* (toward CO<sub>2</sub>), calculated as the molar ratio of CO<sub>2</sub> and CH<sub>4</sub> removed from the gas phase (see Eq. (2)). *S* is expressed in mole of CO<sub>2</sub> per mol of CH<sub>4</sub>. The higher the selectivity, the greater the efficiency of the CO<sub>2</sub> separation process.

$$S = \frac{\text{CO}_2^r}{\text{CH}_4^r} \quad (2)$$

- *t*<sub>50</sub> is the time (in minutes) needed to capture 50% of the total quantity of gas removed. Time *t*<sub>0</sub> is defined as the start of the batch experiment (i.e. when reactor loading is complete) and is equal to *t*<sub>0</sub> = 0 in what follows.
- *t*<sub>90</sub> is the time (in minutes) needed to capture 90% of the total quantity of gas removed.
- *dn/dt* (expressed in mol per min) is the maximum value of the gas enclathration rate during hydrate formation.

## 3. Materials and methods

### 3.1. Additives and materials used

Seven hydrate promoters were chosen: two anionic and one cationic surfactants: sodium dodecyl sulfate (SDS), sodium dodecyl benzene sulfonate (SDBS) and dodecyl trimethyl ammonium chloride (DATCl); and four 5-membered cyclic organic compounds: tetrahydrofuran (THF), 1,3-dioxolane (DIOX), 2-methyl-tetrahydrofuran (m-THF) and cyclopentane (CP). Information on these additives is provided in Table 1.

THF, DIOX and CP are well known to form hydrates of structure (sII), where the 5<sup>12</sup> cavities are empty and the 5<sup>12</sup>6<sup>4</sup> cavities are occupied by the organic molecules [3]. In addition, a number of studies carried out with m-THF and CH<sub>4</sub> [28,29] have demonstrated that the hydrate formed was of structure (sH). It is supposed here that m-THF forms also a structure (sH) in the presence of CO<sub>2</sub> or a CO<sub>2</sub>–CH<sub>4</sub> gas mixture. This assumption is reinforced by the fact the formation of mixed hydrates with THF and

**Table 1**  
Information on the additives used in this study.

Type	Molecule	Name	Structure	Molecular formula	Purity (%)	Supplier
Kinetic additives	SDS	Sodium dodecyl sulfate		NaC <sub>12</sub> H <sub>25</sub> SO <sub>4</sub>	>98	Chem Lab
	SDBS	Sodium dodecyl benzene sulfonate		NaC <sub>18</sub> H <sub>29</sub> SO <sub>3</sub>	88	Acros Organics
	DATCI	Dodecyl trimethyl ammonium chloride		C <sub>15</sub> H <sub>34</sub> ClN	98	Acros Organics
Thermodynamic additives	THF	Tetrahydrofuran		C <sub>4</sub> H <sub>8</sub> O	>99.9	Sigma-Aldrich
	CP	Cyclopentane		C <sub>5</sub> H <sub>10</sub>	99	Acros Organics
	DIOX	1,3-Dioxolane		C <sub>3</sub> H <sub>6</sub> O <sub>2</sub>	99.5	Alfa-Aesar
	m-THF	2-Methyl tetrahydrofuran		C <sub>5</sub> H <sub>10</sub> O	>99	Acros Organics

CH<sub>4</sub>, CO<sub>2</sub> or CH<sub>4</sub> + CO<sub>2</sub> always leads to the same hydrate (sII) structure [15]. To check this hypothesis, it would be very interesting to perform a XRD characterization of the hydrate formed in the presence of m-THF. Unfortunately, we do not have such apparatus and this structural determination is considered out of the scope of this work. For each thermodynamic additive tested (THF, DIOX, CP and m-THF), two concentrations were used: (i) a *low* concentration equal to 4 wt%; (ii) a *high* concentration corresponding to the stoichiometry of the hydrate of structure (sII) for the THF, DIOX and CP, and of (sH) for the m-THF. The stoichiometric concentrations (expressed in wt%) are equal to 19.6, 18.8, 12.5 and 19.2 for DIOX, CP, m-THF and THF, respectively.

Concerning the kinetic additives, there is two important properties of ionic surfactants which have to be defined: (i) an ionic surfactant is able to micellize when its concentration is higher than its Critical Micellar Concentration (denoted CMC); (ii) it does not form micelles below a temperature called the “Krafft point”, denoted  $T_k$ , at which its solubility becomes equal to its CMC. The CMC and Krafft’s point of each surfactant used in this work (in pure water and under atmospheric pressure conditions) are given in Table 2. The concentrations of the kinetic additives used in this work are from 1470 to 7300 ppm for DATCI, 500 to 4800 ppm for SDS, and from 600 to 5800 ppm for SDBS.

The CO<sub>2</sub>/CH<sub>4</sub> gas mixture used in this work was supplied by Air Liquide (France) with a composition of 75.02 ± 0.50 mol% of CO<sub>2</sub> and 24.98 ± 0.50 mol% of CH<sub>4</sub>. This composition has been chosen to address in priority the separation of CO<sub>2</sub> from gas fields having a very high concentration of CO<sub>2</sub>, such as e.g. those of Natuna or El Trapial fields cited in the introduction. For all experiments, the solutions were prepared using an electronic balance with a precision of ±0.001 g, and with ultra-pure water (resistivity of 18.2 MΩ cm) produced in our laboratory by a water purification system from ELGA Labwater (France).

**Table 2**  
Critical micelle concentration (CMC) and Krafft’s point ( $T_k$ ) of the kinetic additives in pure water and ambient pressure.

Additive (-)	CMC (ppm)	Krafft’s point (K)
SDS	2300 [30]	285 ± 4 [31]
SDBS	420 [32]	<273 [33]
DATCI	5600 [34]	<273 [35]

### 3.2. Experimental apparatus

The pilot rig used to carry out the experiments presented in this study is shown in Fig. 1.

The reactor is a jacketed high-pressure cell with an internal volume of 364.7 ± 0.9 cm<sup>3</sup>, heated and cooled by a propylene glycol solution which circulates into the jacket by means of a thermostatic bath (Polystat 37 from Fisher Scientific). It has two sapphire windows 20 mm in diameter, and is connected to a gas storage vessel with a pressure-reducing valve. Pressure in the cell is measured by a 0–10 MPa pressure transducer with a precision of ±0.02 MPa, and the gas/liquid temperatures are measured with two PT100 probes with a precision of ±0.2 K. Note that these accuracy values integrate the intrinsic error of the sensors, the data acquisition system and the repeatability of the measurements. A gas chromatograph (HP-GC6980 from Agilent), connected to the reactor and equipped with a high pressure sampling system, a capillary column HP-PLOT-Q and a thermal conductivity detector, was used to analyze the gas composition throughout the experiment. The mean error – including the precision of the gas composition analyses and the reproducibility of the experiments – was estimated to be less than 2.0 mol%, and the whole sampling system was optimized to create a negligible pressure drop (less than 0.001 MPa) for each point of analysis. A high-definition camera (Pro 9000 HD webcam from Logitech) was placed in front of one of the reactor windows to provide a direct view of what happened inside the reactor. To ensure efficient solubilization of the gases into the liquid phase, and to enhance thermal transfer, a 20 mm diameter, star-shaped magnetic agitator rotates on the reactor bottom. Note that this agitation system has insufficient torque to be able to stir any hydrate suspension. It is therefore stopped manually by the operator as soon as crystallization is visually detected, and the hydrate growth is always achieved in quiescent – or static – conditions. Data are recorded at a frequency of 1 Hz on a PC via a home-made Lab view<sup>®</sup> interface.

### 3.3. Experimental protocol

A volume of 65.0 ± 0.1 cm<sup>3</sup> of solution containing the additives was first introduced into the reactor, where it reached the middle of the windows. The reactor was then closed, regulated at 293 K, and flushed twice with the CO<sub>2</sub>/CH<sub>4</sub> gas mixture to remove the air initially present in the apparatus. Next, it was quickly

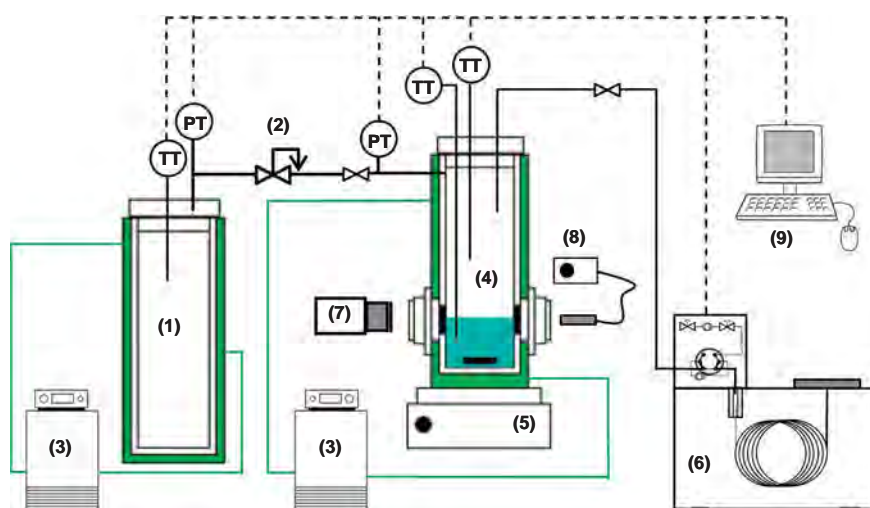


**Fig. 1.** Experimental rig used for the experiments: (1) gas storage vessel; (2) pressure reducing valve; (3) thermostatic baths; (4) hydrate forming reactor; (5) magnetic agitator; (6) high pressure gas chromatograph; (7) CCD camera; (8) lighting system of the reactor; and (9) standard PC for data acquisition.

pressurized to the desired pressure (denoted  $P_{load}$ ), during which time (with the agitator off) the quantity of gas which dissolves in the liquid was negligible [27]. The gas feeding valve was then closed to operate the reactor in batch conditions till the end of the experiment. Agitation was started and maintained at 600 RPM for 120 min to solubilize the gas into the solution. The reactor was then cooled at a rate of 0.9 K/min from 293 K to the target temperature (denoted  $T_{targ}$ ) of 275 K, after which the system was maintained at this temperature to form hydrates. Finally, the temperature was raised to 293 K again to dissociate all the hydrates formed.

## 4. Results

### 4.1. Detail of a typical experiment

A typical experiment, carried out with a combination of SDS and DIOX is shown in Fig. 2, and briefly discussed in this section.

From the beginning of the experiment to point A, the reactor pressure decreased as the gas (mainly the  $\text{CO}_2$ ) solubilized into the solution, and then stabilized (at point A) when the solubility equilibrium was reached. From point A to B, the reactor was cooled until the target temperature  $T_{targ}$  was reached. In some cases, the solution which was initially transparent (see Snapshot A) became turbid (see Snapshot B) owing to the precipitation of the surfactant (e.g. SDS) at this temperature. At point C, a first bulk hydrate crystallization occurred in the mixture (see snapshot C), accompanied by a first temperature peak clearly visible in Fig. 2(a) and (c). It is attributed to the formation of a mixed hydrate containing both the thermodynamic additive used (here the DIOX) and the gases ( $\text{CO}_2$  and/or  $\text{CH}_4$ ) [26,36,37]. The hydrate crystals then promote a second hydrate crystallization, which starts at point D in Fig. 2. This is attributed to the formation of the  $\text{CO}_2$ - $\text{CH}_4$  binary hydrate. It led to another temperature increase (see inside the dashed rectangle labeled by  $\star$ , drawn in Fig. 2(a)), a rapid gas pressure decrease (Fig. 2(a)), a substantial gas uptake and a significant decrease in the  $\text{CO}_2$  composition of the remaining vapor phase (see Fig. 2(b)). Note that the temperature peak resulting from the exothermicity of the second hydrate formation reached a maximum value at point E, correlated in our previous studies to the maximum value of the gas enclathration rate [26,38]. Then, the reactor pressure stabilizes at point F, on the three-phase (Liquid-Hydrate-Vapor) equilibrium line (see Fig. 2(b)). The experimental

pressure measured at point F very closely matches the equilibrium pressure predicted by both the correlation of Adisasmito [39] and the CSMGem program developed by the Colorado School of Mines [3]. Interestingly, the period from points E to F – and particularly near point E – is always characterized by a rapid propagation, through the mass of crystals already present in the bulk, of dark efflorescences as shown in Snapshots E and F. Finally, during the dissociation stage (from point F to I), we frequently noted small “accidents or bumps” in the experimental curves (e.g. points G and H on Fig. 2(a) and (c)), which may correspond to the gradual dissociation of the two hydrates formed. However, a very slow dissociation ramp, about  $\sim 0.1$  K/hour or less [40] would be necessary to precisely determine the position of the phase transition points, and cannot be obtained with the experimental apparatus used here). The precise analysis of the dissociation curve is outside the scope of this work.

### 4.2. Comparison of the kinetic additives

To perform the tests with the different kinetic additives in combination with a thermodynamic promoter, THF was chosen as a reference and used at 4 wt% in water. This concentration was defined from the results of a previous author’s study carried out with pure  $\text{CO}_2$ , demonstrating that it allowed an efficient gas enclathration process, with a high water-to-hydrate conversion, even in static conditions [25].

The effect of the nature of the kinetic additives on the enclathration process performance was examined through experiments carried out with SDS, SDBS or DATCI used at a concentration of 3000 ppm. The loading pressure  $P_{load}$  was 4.0 MPa. The results obtained and the morphology of the hydrate observed at the end of the experiments are presented in Fig. 3. The experimental dataset is summarized in Table 3.

The temperature peaks noted in Fig. 3(b) are evidence of the formation of the mixed hydrate containing THF, which always forms first (as already discussed above in Section 4.1).

With SDS or SDBS, a significant drop in the reactor pressure was observed after 160 min (Fig. 3(a) and (c)), indicating that a large quantity of gas had been removed from the gas phase (more than 55% of the initial quantity). For both additives, the averaged value of the pressure reached at the end of the experiments was  $1.85 \pm 0.01$  MPa. This matches the equilibrium pressure of the binary  $\text{CO}_2$ - $\text{CH}_4$  hydrate at 275 K, calculated at the averaged

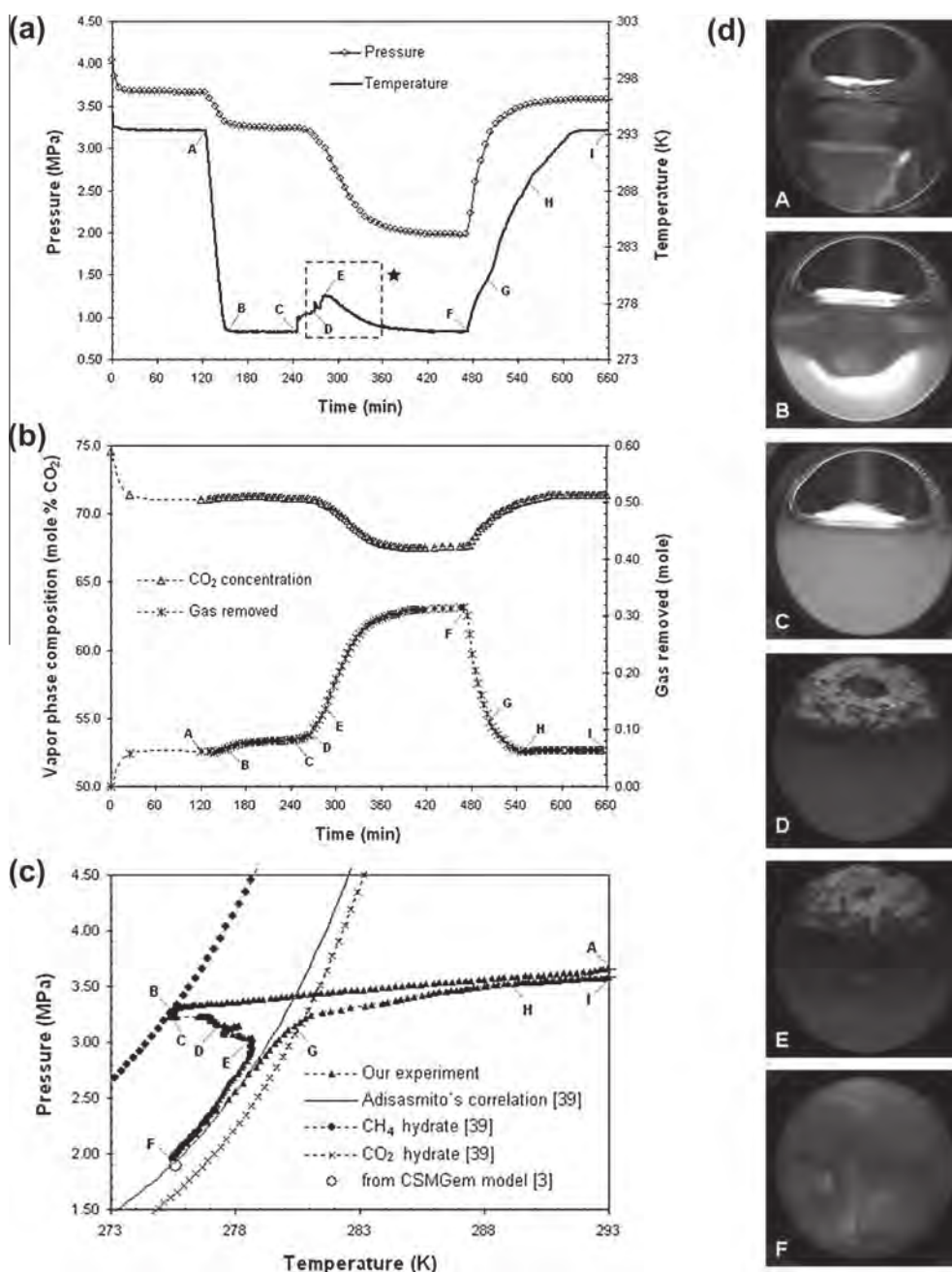


**Fig. 2.** Type curves obtained for the system SDS (3000 ppm) + DIOX (4 wt%),  $P_{load} = 4.0$  MPa and  $T_{target} = 275$  K. (a) reactor pressure and temperature versus time, ★ area of interest highlighting the temperature increase; (b) gas composition and quantity of gas removed versus time; (c) corresponding  $P$ - $T$  diagram with our experiment and HLV equilibrium data from literature; and (d) snapshots.

measured final gas composition  $y_{CO_2} = 67.6 \pm 0.5$  mol% (see Fig. 3(d)) with Adisasmith's correlation [39]. This point demonstrates, corroborating previous findings with pure CO<sub>2</sub> hydrates [25], that SDS (and likewise SDBS here) used at this concentration has no detectable influence on the hydrate equilibrium conditions. Regarding the indicators of the enclathration kinetics (defined in Section 2), the process is more efficient when SDS is used rather than SDBS (see Table 3):  $t_{50}$  and  $t_{90}$  are slightly reduced by about 5%, while the  $dn/dt$  is increased by about 29.0% (values calculated in reference to the SDS data). However, at concentrations of 3000 ppm and higher, a selectivity close to  $S = 4$  mol CO<sub>2</sub>/mol CH<sub>4</sub>, and almost identical for the two additives, was found.

With DATCI, the results, plotted in Fig. 3(a), indicate a very different behavior from the system. The reactor pressure obtained at

the end of the experiment ( $P_r = 3.29$  MPa) was almost equal to the equilibrium pressure ( $P_r = 3.30$  MPa) obtained by using only THF (i.e. without any kinetic additive present in the system), leading to removal of only 0.073 mol of gas (12.0%) as illustrated in Fig. 3(c). Several experiments were carried out with different concentrations of DATCI. They were left for longer than 24 h under agitation at 275 K without any significant increase in the quantity of gas removed being observed. In addition, the appearance of the hydrates formed with this additive differed from the cases where SDS or SDBS were used. The bulk appears visually much more compact, and no dark efflorescence was observed during the experiment. No apparent change in the hydrate appearance was noted from the time the first mixed hydrate was formed through to the end of the experiment: it was as if the enclathration process "stopped",

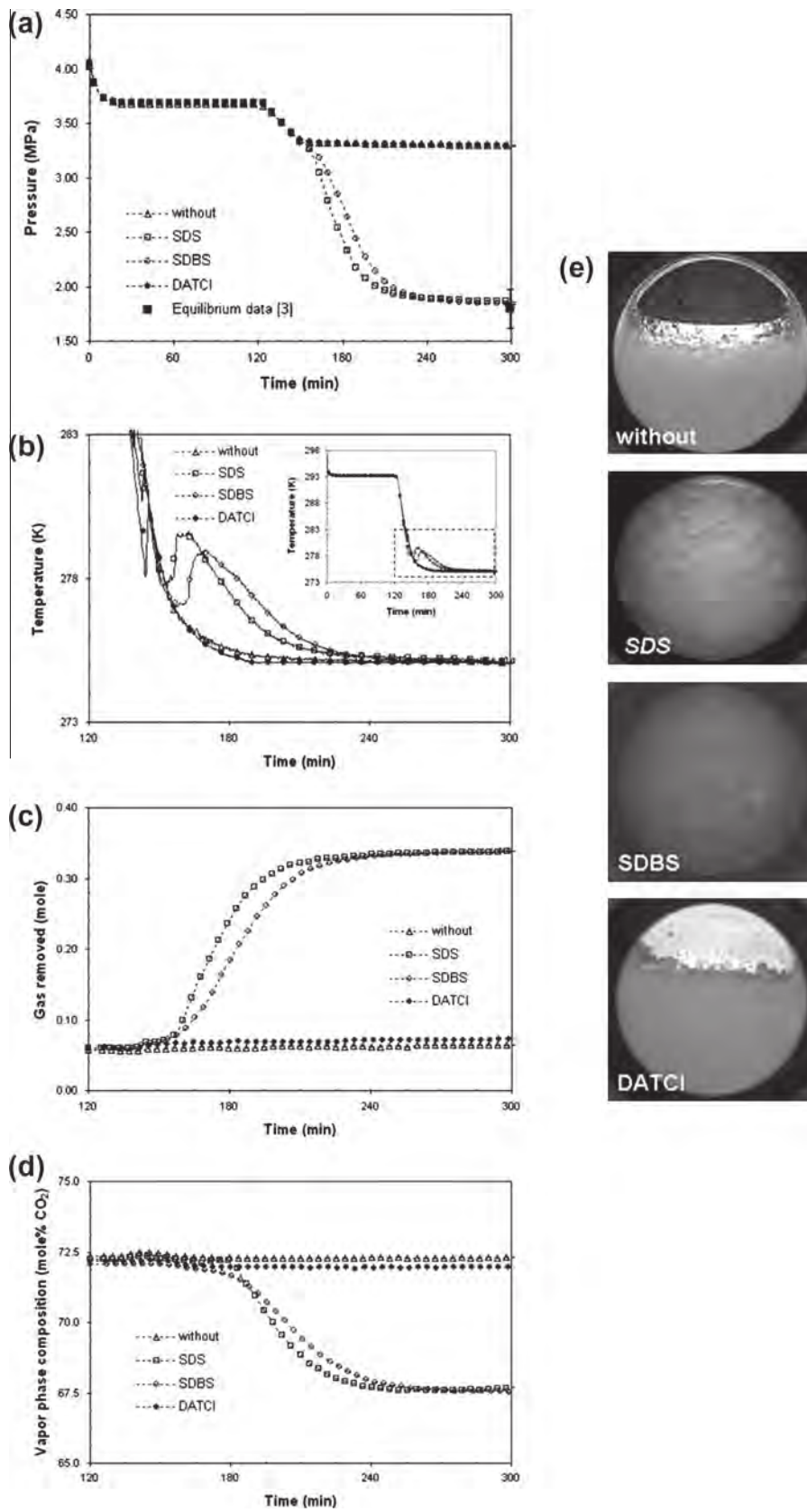


**Fig. 3.** Comparison of the kinetic additives: (a) reactor pressure versus time; (b) reactor temperature versus time; (c) quantity of gas removed versus time; (d) vapor phase composition versus time (e) snapshots taken at the end of the hydrate formation. The system contains 3000 ppm of the kinetic additive and 4 wt% of THF;  $P_{load} = 4.0$  MPa and  $T_{target} = 275$  K.



**Table 3**Results obtained by combination of a kinetic additive (SDBS, DATCl and SDS) at different concentration with THF used at 4 wt%.  $P_{load} = 4.0$  MPa and  $T_{target} = 275$  K.

Additive (-)	Equilibrium conditions								
	Additive (wt%)	$P_{exp}$ (MPa)	$y_{CO_2}$ (mol%)	Gas removed		Selectivity ( $n_{CO_2}/n_{CH_4}$ )	$t_{50\%}$ (min)	$t_{90\%}$ (min)	$dn/dt * 10^3$ (mole/min)
Without	0	3.30	72.3	0.064	10.6	13.1	-	-	-
SDBS	600	3.27	72.1	0.074	12.2	12.8	-	-	-
	1930	3.28	71.8	0.076	12.5	12.9	-	-	-
	3000	1.84	67.5	0.339	55.9	4.0	178	207	4.661
	3620	1.83	67.8	0.336	55.7	4.0	176	198	4.659
	5800	1.86	67.9	0.332	55.2	3.9	168	210	4.735
DATCl	1470	3.30	72.1	0.069	11.3	13.5	-	-	-
	2745	3.29	72.0	0.067	11.5	12.8	-	-	-
	3000	3.29	72.3	0.073	12.0	12.8	-	-	-
	7300	3.29	72.1	0.072	11.8	12.9	-	-	-
SDS <sup>a</sup>	500	1.82	67.2	0.337	56.4	4.0	356	389	4.563
	1000	1.88	67.1	0.336	55.1	4.1	185	214	5.645
	1600	1.84	67.3	0.340	55.9	4.0	179	207	6.503
	3000	1.86	67.7	0.338	55.5	3.9	169	198	6.572
	4800	1.87	68.2	0.332	54.9	3.8	174	210	5.642

<sup>a</sup> From Ricaurte et al. [26].

as soon as the first mixed hydrate was formed. DATCl was therefore considered as not efficient at promoting the formation of the binary CO<sub>2</sub>-CH<sub>4</sub> hydrate (i.e. leading to a significant drop in reactor pressure). As very little hydrate was formed, the selectivity of the separation remains high ( $S = 12.8$ ), due mainly to the higher solubility of the CO<sub>2</sub> in the solution than the CH<sub>4</sub> (see Table 3). This value of  $S$  is comparable to that obtained without kinetic additive ( $S = 13.1$ ). Therefore, it can be concluded that, although DATCl is an ionic surfactant, this additive is not acting as a kinetic promoter for this system.

Considering only the two kinetic additives that were found to enhance the enclathration process (i.e. SDS and SDBS) used in combination with THF at 4 wt%, the effect of the kinetic additives' concentration is reported in Fig. 4. Note that Fig. 4 shows the normalized enclathration rate, which is a non-dimensionalised fraction where the normalization factor is the number of moles of gas initially present (denoted  $n_0$ ), versus time. The enclathration rate was found to be enhanced by the presence of SDS in concentrations ranging from 500 to 4800 ppm:  $(dn/dt)/n_0$  increased with the SDS concentration, reached a plateau between  $\sim 1600$  and  $\sim 3000$  ppm and decreased at higher concentrations. With SDBS, several differences were noted: (i) no effect was obtained at the lowest concentrations tested (600 and 1930 ppm); (ii) from 3000 to 5800 ppm, the enhancement effect was obtained and the resulting enclathration rate was nearly constant. One interesting point is that the enclathration rates obtained using SDS are always superior to those obtained with SDBS. However, the hydrate morphologies observed during the experiment were identical (i.e. hydrates grew along the reactor window, and dark efflorescences in the bulk correlated with a dramatic drop in the reactor pressure). The appearance of the bulk at the end of the experiment was consequently very similar to these two additives shown previously in Fig. 3(e). These two anionic surfactants probably have a similar mechanism for enhancing hydrate formation.

However, the action mechanisms of these surfactants are not yet fully understood, as the system investigated is relatively complex. It is worth noting that, in this work, the temperature at which the CO<sub>2</sub>-CH<sub>4</sub> binary hydrate forms (275 K) is lower than the Krafft's point of SDS (see Table 2). In these conditions, one would expect the sudden precipitation of the SDS at low temperature to trigger crystallization of the binary CO<sub>2</sub>-CH<sub>4</sub> hydrate. But the hydrate formation temperature of 275 K is higher than the Krafft's point of SDBS (which is lower than 273 K as indicated in Table 2). So SDBS is unlikely to precipitate at this temperature: this point

was confirmed experimentally, as the aqueous phase remains transparent at temperature  $T_{target}$  when this additive is used alone. Therefore, this option is not the correct one to explain why SDS and SDBS are both good kinetic promoters. Moreover, high-rate gas enclathration is obtained for surfactant concentrations either lower (for SDS) or higher (for SDS and SDBS) than the CMC of each surfactant. Accordingly, there would appear to be no direct correlation between the presence of micelles in the solution and the enclathration process efficiency (i.e. to obtain a large pressure drop with enclathration at high rate). This assumption is supported by various authors [30,41]. Therefore, the presence of micelles is unlikely to be the parameter which controls the ability of the additive to enhance the hydrate formation kinetics.

Our main assumption, in the conditions of this work, is that a "good kinetic promoter" (i.e. comparable to SDS or SDBS) may adsorb both on the surface of the mixed hydrate (containing in this instance THF) that first formed into the bulk, and on the CO<sub>2</sub> hydrate. The adsorption of SDS on the surface of pure (sl) hydrates has already been demonstrated experimentally with cyclopentane [42] and THF [43]. Adsorption (of surfactants on hydrate surfaces) may prevent the hydrate particles from agglomerating into large compact masses and allow a network of hydrate particles to build up, wettable to water, and able to "suck" – or "pump" – the remaining aqueous solution by capillarity. This porous hydrate structure would maintain a high exchange surface between the gas phase and the water phase, even in quiescent conditions. This "capillary-driven" mechanism was observed experimentally by others with SDS and hydrocarbon gas mixtures [21], and can be related to the observations made by various authors who have shown (at the end of the experiment) an annular hydrate layer which has grown up along the reactor walls [25,44].

#### 4.3. Comparison of thermodynamic additives

SDS was chosen as the reference kinetic additive to perform the experiments with the thermodynamic promoters – as it appears to be the most efficient of the three kinetic additives tested – and used at a concentration of 3000 ppm which was found to maximize the enclathration rate with THF. The gas loading pressure of the reactor was also varied from 3.0 to 4.0 MPa. The experimental dataset is given in Table 4.

The results obtained using the different thermodynamic additives at 4 wt% combined with 3000 ppm of SDS and with  $P_{load} = 4.0$  MPa, are shown in Fig. 5.

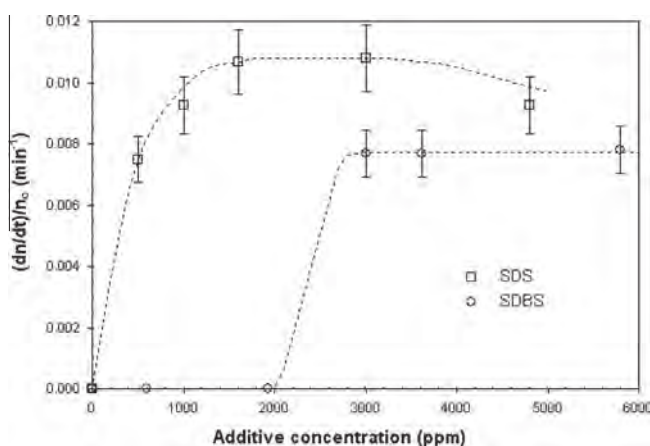


**Fig. 4.** Influence of the concentration of SDS and SDBS on the gas enclathration rate. The conditions are: concentration of THF = 4 wt%;  $P_{load} = 4.0$  MPa and  $T_{targ} = 275$  K.  $n_o$  is the number of moles of gas initially present.

For the system without any thermodynamic additive, no hydrate formation is observed, as expected. Only SDS precipitation occurs (see the upper snapshot in Fig. 5(e)).

For the DIOX, CP and THF additives, the two successive hydrate crystallizations are clearly observed, following the mechanism described in the Section 4.1. The observations made during the experiment were also identical for the three additives: the hydrates grow up the reactor window, and dark efflorescences (correlated with the enclathration of gas at high rate) appear throughout the crystals already present in the bulk. So the appearance of the system at the end of the experiments is very similar for the three additives, as can be seen from the snapshots in Fig. 5(e). As shown in Fig. 5(a), at low additive concentration, the reactor pressure obtained at the end of the experiment is the same for DIOX, CP and THF. The experimental pressure value reached by the system matches the equilibrium pressure of the  $\text{CO}_2$ - $\text{CH}_4$  hydrate at this temperature and gas composition (see Fig. 5(c) and (d)). As shown in Fig. 5(b), the quantity of gas removed increases with the loading pressure of the reactor, as more binary  $\text{CO}_2$ - $\text{CH}_4$  hydrate is formed.

However, at each level of pressure considered, the quantity of gas removed and the selectivity of the separation was found to be of the same order of magnitude for all three additives (see Table 4). Interestingly, when the gas loading pressure decreases (e.g. from 4.0 to 3.0 MPa), the selectivity toward  $\text{CO}_2$  increases (e.g. by 33% for CP), while the quantity of gas removed decreases (e.g. by 28% for CP). For the conditions investigated in this work, as the water to hydrate conversion always ends when the hydrate equilibrium is reached, a lower loading pressure leads necessarily to less hydrate being formed and hence to more free water remaining. Therefore, few hydrates formed leads to little gas removed, and more free water leads to higher selectivity (as the solubilization of  $\text{CO}_2$  in water is much higher than for  $\text{CH}_4$ ).

An exception is observed for DIOX at the lowest pressure tested (3.0 MPa) where only one crystallization took place (and a very small temperature peak was observed). This particular behavior is attributed to a combination of lower DIOX promoting effect at this concentration (compared to THF or CP) and a low pressure condition.

Similarly to the case where no thermodynamic additive is used, Fig. 5 shows clearly that no hydrate was formed with m-THF (even when, in a complementary experiment, the target temperature was decreased to 273.7 K and the system left at this temperature for more than 16 h under agitation). The final pressure was found to be the same as when no thermodynamic additive was present. To the best of the author's knowledge, no data is available in the literature for the system  $\text{CH}_4$ - $\text{CO}_2$ -(m-THF). However, a number of studies carried out with only m-THF and  $\text{CH}_4$  have demonstrated that the corresponding hydrate equilibrium curve (obtained with 2.9 mol% of m-THF and  $\text{CH}_4$ ) is close to that of pure methane hydrate [28,29]. In addition, a study of the  $\text{CH}_4$ - $\text{CO}_2$ -neohexane system based on  $\text{CO}_2$  concentrations in gas close to that used in our work shows that the equilibrium conditions of the (sH) structure formed in presence of neohexane undergo little impact compared to the  $\text{CO}_2$ - $\text{CH}_4$  system which forms (sl) [45]. Therefore, it can be stated that m-THF is likely to be a weak thermodynamic promoter, and the driving force applied on the system in our experiments was insufficient to induce (sH) hydrate crystallization. Interestingly, when m-THF is present, no SDS precipitation was observed, as can be seen in Fig. 5(d) where the solution remains transparent.

**Table 4**

Results obtained (different reactor loading pressures) by combination of a thermodynamic additive (DIOX, CP, m-THF and THF) at different concentration with SDS used at 3000 ppm;  $T_{targ} = 275$  K.

Additive (-)	Equilibrium conditions									
	Additive (wt%)	$P_{load}$ (MPa)	$P_{exp}$ (MPa)	$y_{\text{CO}_2}$ (mol%)	Gas removed (mole) (%)		Selectivity ( $n_{\text{CO}_2}/n_{\text{CH}_4}$ )	$t_{50\%}$ (min)	$t_{90\%}$ (min)	$dn/dt * 10^3$ (mole/min)
Without	0	4.00	3.24	71.1	0.084	13.8	27.0	-	-	-
DIOX	4.0	3.00	2.20 <sup>a</sup>	70.7 <sup>a</sup>	0.104 <sup>a</sup>	24.1 <sup>a</sup>	6.6 <sup>a</sup>	-	-	-
	4.0	3.50	1.94	67.9	0.232	45.1	4.9	361	438	1.740
	4.0	4.00	1.97	67.7	0.315	52.2	4.2	290	360	2.863
	19.6	4.00	2.89	71.3	0.150	24.8	5.3	153	212	2.462
CP	4.0	3.00	1.84	68.1	0.161	37.6	6.1	167	209	2.007
	4.0	3.50	1.91	67.1	0.241	46.3	5.1	173	214	3.255
	4.0	4.00	1.95	66.5	0.315	52.5	4.6	178	231	3.965
	18.8	4.00	2.59	70.3	0.210	34.5	4.8	152	194	2.050
m-THF	4.0	3.00	2.41	70.7	0.063	14.6	36.9	-	-	-
	4.0	3.50	2.28	70.9	0.072	14.0	25.7	-	-	-
	4.0	4.00	3.23	71.1	0.085	14.1	25.0	-	-	-
	12.5	4.00	3.20	69.7	0.105	17.0	53.7	-	-	-
THF <sup>b</sup>	4.0	3.00	1.85	68.5	0.160	37.2	5.2	168	200	2.398
	4.0	3.50	1.85	67.2	0.225	45.5	4.8	170	201	3.329
	4.0	4.00	1.86	67.7	0.338	55.5	3.9	169	198	6.572
	19.2	4.00	2.82	71.7	0.168	27.6	4.6	136	176	3.718

<sup>a</sup> Values after 24 h of experiment.

<sup>b</sup> From Ricaurte et al. [26].

The effect of the additive concentration is analyzed through the results presented in Figs. 6 and 7. Fig. 6 shows a representative example of the evolution of the reactor pressure, temperature and gas phase composition versus time at a “low” and “high”

concentration of additive. DIOX was chosen as an example in Fig. 6 for its ready correlation with the data presented in Fig. 2, but the same behavior was noted for all the additives, except mTHF with which no hydrate forms. At high concentration

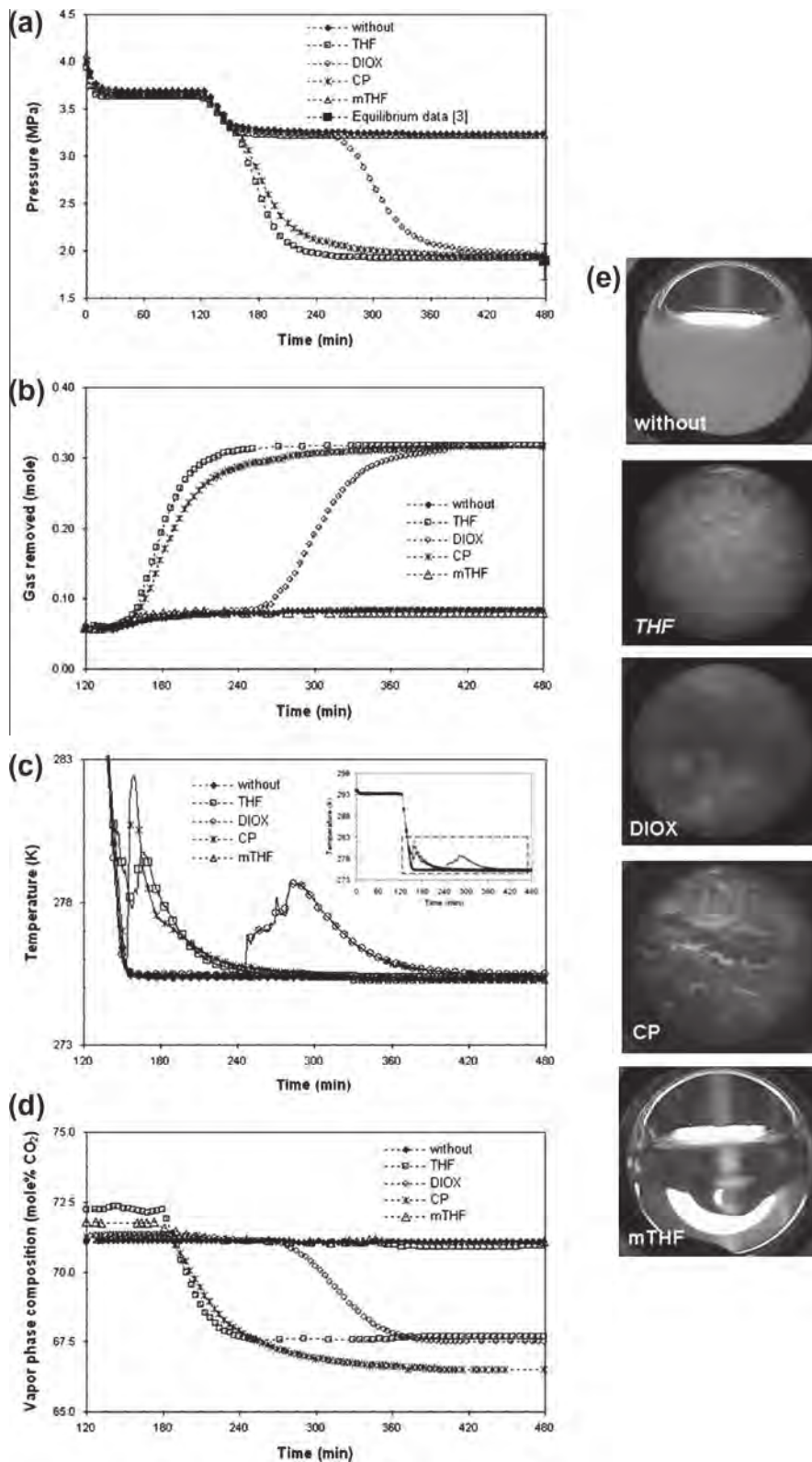


**Fig. 5.** Comparison of the thermodynamic additives: (a) reactor pressure versus time; (b) reactor temperature versus time; (c) quantity of gas removed versus time; (d) vapor phase composition versus time; and (e) snapshots taken at the end of the hydrate formation. The system contains 4 wt% of the thermodynamic additive and 3000 ppm of SDS;  $P_{load} = 4.0$  MPa and  $T_{targ} = 275$  K.

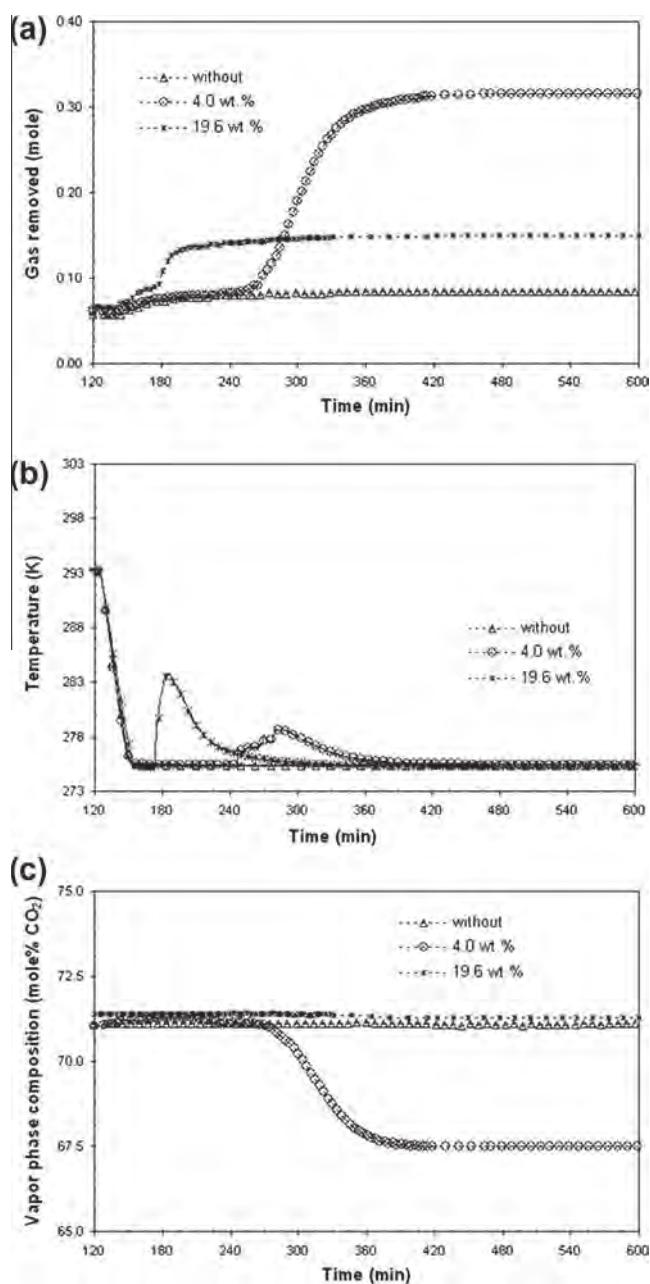


**Fig. 6.** Example showing the influence of the thermodynamic additives concentration (here the DIOX): (a) quantity of gas removed versus time; (b) reactor temperature versus time; and (c) vapor phase composition versus time. The SDS concentration is fixed to 3000 ppm.

(19.6 wt% of DIOX), the quantity of gas removed is less than half that obtained at low concentration (4 wt% of DIOX). A single and very large temperature peak (about 9 K of magnitude) is measured (see Fig. 6(b)). The fact that no secondary crystallization is observed suggests that most of the water and DIOX is consumed to form the mixed hydrate. It is clearly apparent in Fig. 7 that the quantity of removed gas obtained at low concentration (4 wt%) is between 60% and 100% higher than at high concentration. In addition, for DIOX, THF or CP (with the same reactor loading pressure, of 4.0 MPa for the data in Fig. 7), the selectivity of the separation did not greatly vary (i.e. from 3.9 for THF to 4.6 for CP moles of CO<sub>2</sub> per mole of CH<sub>4</sub>, in these conditions). However, an exception is noted for the experiments with m-THF, where the selectivity was more than doubled at high concentration ( $S$  increases from 25.0 to 53.7). This result is explained by the fact that, just as

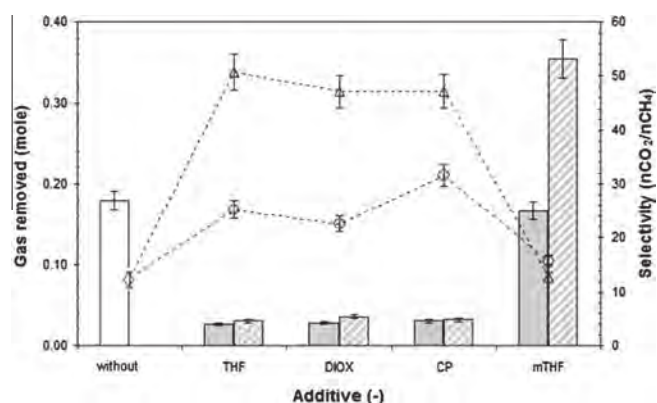


**Fig. 7.** Comparison of the thermodynamic additives, used at low (4 wt%) and high (stoichiometric) concentrations in combination with SDS at 3000 ppm, on the quantity of gas removed and the selectivity. Gas removed (symbols):  $\diamond$  without additive;  $\triangle$  4 wt%;  $\circ$  stoichiometric concentration. Selectivity (bars): white is without additive; grey is for 4 wt%; hatching is for stoichiometric concentration.

stoichiometric aqueous solutions of THF forms two liquid phases in presence of CO<sub>2</sub> [46], the stoichiometric solutions of m-THF in our experiment exhibit the same behavior in the presence of CO<sub>2</sub>. As CO<sub>2</sub> is generally highly soluble in ethers [47], the global selectivity of the process is greatly increased due to the preferential solubilization of the CO<sub>2</sub> in the pure m-THF.

Finally, in previous recent studies of the author carried out with the combination of THF + SDS and CO<sub>2</sub> + CH<sub>4</sub> [26] at various concentrations of THF and 3000 ppm of SDS, the concentration of THF initially present in the bulk – even if almost all this additive is found in the mixed hydrate which crystallizes first – was found to significantly impact the formation kinetics of the second hydrate (the binary CO<sub>2</sub>-CH<sub>4</sub> hydrate or the pure CO<sub>2</sub> hydrate). Consequently, the comparison of the kinetic performance of these three additives coupled with the resulting selectivity, is a key point of this study. Our data analysis suggests that, in our case: (i) THF is the additive with which the mixed hydrate forms soonest; (ii) when the binary CO<sub>2</sub>-CH<sub>4</sub> hydrate starts to crystallize, the use of THF helps it form at the higher rate; (iii) when hydrates are formed, the selectivity  $S$  of the separation is equivalent with DIOX, CP and THF, and the average value of  $S$  is about 4 mol of CO<sub>2</sub> per mole of CH<sub>4</sub>; (iv) if we were asked to rank the four thermodynamic additives tested in decreasing order of kinetic performance, our classification would be: THF > CP > DIOX  $\gg$  m-THF (as this last additive did not induce the formation any hydrate under the experimental conditions of this study).

## 5. Concluding remarks

This study investigates the effect of a combination of thermodynamic additives and kinetic additives on hydrate formation, where three ionic surfactants (SDS, SBBS and DATCI) and four cyclic organic compounds (DIOX, CP, THF and m-THF) were tested, in various combinations.

The global action mechanism is identical for most of the combinations tested. At low concentrations of the thermodynamic promoter (i.e. 4 wt%), the system first forms a mixed hydrate containing the organic compound which, when the subcooling conditions are appropriate, triggers formation of the binary CO<sub>2</sub>-CH<sub>4</sub> hydrate. An exception was found for m-THF which did not form any hydrate under the various experimental conditions tested in this work, probably due to its weak promoting effect and its ability to induce hydrates of structure (sH).

Concerning kinetic additives, our ranking would be: SDS > SBBS  $\gg$  DATCI (in combination with THF) to enhance the hydrate formation rate of the CO<sub>2</sub>-CH<sub>4</sub> binary hydrate, with a

$(dn/dt)_{\max}$  for the system THF + SDS of about  $6.6 \times 10^{-3}$  mol of gas per min. However, the action mechanism of the surfactants used is not fully understood to date.

Concerning thermodynamic additives, the nature of the organic compound also influences the hydrate formation kinetics of the CO<sub>2</sub>-CH<sub>4</sub> binary hydrate, even if the organic molecule is already crystallized in the bulk in the form of mixed hydrates. The best results in terms of hydrate formation kinetics for the binary CO<sub>2</sub>-CH<sub>4</sub> hydrate were thus obtained using the additives at low concentration (4 wt%), leading for example to a reduction of about 90% of the  $t_{50}$  for the system DIOX + SDS if the concentration of DIOX is decreased from 19.6 to 4 wt%. THF appears to be the most efficient, both in reducing the induction time of the mixed hydrate and in enhancing the hydrate formation rate, e.g. by increasing it of a factor 1.6 and 2.3 the enclathration rate obtained using CP, and DIOX in the same conditions, respectively. Therefore, our classification of the thermodynamic additives (in combination with SDS) would be THF > CP > DIOX  $\gg$  m-THF.

In terms of selectivity of separation, the combination of a kinetic additive and a thermodynamic additive produces values of  $S$  close to 4 molecules of CO<sub>2</sub> per mole of CH<sub>4</sub>.

In terms of technology transfer from the lab to larger scale, the gas enclathration rate is still to low – in the conditions tested in this work – to foresee any scale-up to date. One reason would be that the multiphasic contactor used in the experiments is not efficient in terms of mass transfer, as the crystallization is done in quiescent conditions (the worst case). It would be interesting to study and compare different technological options, more advantageous in terms of hydrodynamics and/or heat and mass transfers, such as agitated reactors, bubbles columns, and slurry loop reactors. Similarly, the low selectivity value toward CO<sub>2</sub> is another important limitation, which remains to be unlocked (e.g. by using novel additives or a multi-stage process) if any application of this technique for CO<sub>2</sub>/CH<sub>4</sub> separation at industrial scale is to be expected.

The coupling of additives, and particularly the association of a kinetic and a thermodynamic additive, has proved to be a promising method to enhance hydrate formation kinetics and shorten induction times. However, the action mechanisms still need closer investigation to understand, in particular, the action of the surfactant, and to determine how the synergies work. In situ spectroscopic measurements (e.g. by using Raman analysis) or microscopic observations of the crystals (e.g. by using a Particle Video Microscope) during hydrate formation could bring valuable elements to go further in the mechanisms. Unfortunately, we do not have yet the experimental apparatuses to perform such analyses. As more efficient combinations of additives doubtless exist, the search for substitute compounds of THF remains of paramount importance for many practical applications. However, the system based on SDS + THF remains to date the most efficient additive combination found in the scope of this work.

## Acknowledgements

Joseph Diaz is particularly acknowledged for his work and assistance on the experimental rigs. The staff of the “Atelier de Physique” of the University of Pau is also thanked. The authors are grateful to Total E&P (“Gas Solutions” R&D Project), Fundayacucho from Venezuela and CG64 (Conseil Général des Pyrénées Atlantiques) for financial support of this work.

## References

- [1] Sloan ED. *Fundamental principles and applications of natural gas hydrates*. Nature 2003;426:353–9.
- [2] Koh CA. Towards a fundamental understanding of natural gas hydrates. Chem Soc Rev 2002;31:157–67.

- [3] Sloan ED, Koh CA. *Clathrate hydrates of natural gases*. 3rd ed. New York: CRC Press; 2008.
- [4] Sun C, Li W, Yang X, Li F, Yuan Q, Mu L, et al. Progress in research of gas hydrate. Chin J Chem Eng 2011;19:151–62.
- [5] Eslamimanesh A, Mohammadi AH, Richon D, Naidoo P, Ramjugernath D. Application of gas hydrate formation in separation processes: a review of experimental studies. J Chem Thermodyn 2012;46:62–71.
- [6] Sabil KM, Azmi N, Mukhtar H. A review on carbon dioxide hydrate potential in technological applications. J Appl Sci 2011;11:3534–40.
- [7] Tajima H, Yamasaki A, Kiyono F. Energy consumption estimation for greenhouse gas separation processes by clathrate hydrate formation. Energy 2004;29:1713–29.
- [8] Duc NH, Chauvy F, Herri J-M. CO<sub>2</sub> capture by hydrate crystallization – a potential solution for gas emission of steelmaking industry. Energy Convers Manage 2007;48:1313–22.
- [9] Economides MJ, Oligney RE, Lewis PE. U.S. Natural gas in 2011 and beyond. J Nat Gas Sci Eng 2011;2012(8):2–8.
- [10] Kidnay AJ, Parrish WR, McCartney DG. *Fundamental of natural gas processing*. 2nd ed. Boca Raton: CRC Press; 2011.
- [11] Hanif A, Suhartanto T, Green MLH. Possible utilisation of CO<sub>2</sub> on natura's gas field using dry reforming of methane to syngas (CO + H<sub>2</sub>). In: SPE – Asia Pacific Oil and Gas Conference, 8–10 October 2002, Melbourne, Australia. p. 833–40.
- [12] Crotti MA, Fernandez G, Terrado M. Improving reserves and production using a CO<sub>2</sub> fluid model in El Trapial field, Argentina. In: Latin American & Caribbean petroleum engineering conference, 15–18 April 2007, Buenos Aires, Argentina. p. 1008–015.
- [13] Rufford TE, Smart S, Watson GCY, Graham BF, Boxall J, Diniz de Costa JC, et al. The removal of CO<sub>2</sub> and N<sub>2</sub> from natural gas: a review of conventional and emerging process technologies. J Petrol Sci Eng 2012;94–95:123–54.
- [14] van Denderen M, Ineke E, Golombok M. CO<sub>2</sub> removal from contaminated natural gas mixtures by hydrate formation. Ind Eng Chem Res 2009;48:5802–7.
- [15] Lee Y-J, Kawamura T, Yamamoto Y, Yoon J-H. Phase equilibrium studies of tetrahydrofuran (THF) + CH<sub>4</sub>, THF + CO<sub>2</sub>, CH<sub>4</sub> + CO<sub>2</sub>, and THF + CO<sub>2</sub> + CH<sub>4</sub> hydrates. J Chem Eng Data 2012;57:3543–8.
- [16] Kumar A, Sakpal T, Linga P, Kumar R. Influence of contact medium and surfactants on carbon dioxide clathrate hydrate kinetics. Fuel 2013;105:664–71.
- [17] Zhong D-L, Daraboina N, Englezos P. Recovery of CH<sub>4</sub> from coal mine model gas mixture (CH<sub>4</sub>/N<sub>2</sub>) by hydrate crystallization in the presence of cyclopentane. Fuel 2013;106:425–30.
- [18] Trueba AT, Rovetto LJ, Florusse LJ, Kroon MC, Peters CJ. Phase equilibrium measurements of structure II clathrate hydrates of hydrogen with various promoters. Fluid Phase Equilib 2011;307:6–10.
- [19] Delahaye A, Fourmaison L, Marinhas S, Chatti I, Petitot J-P, Dalmazzone D, et al. Effect of THF on equilibrium pressure and dissociation enthalpy of CO<sub>2</sub> hydrates applied to secondary refrigeration. Ind Eng Chem Res 2006;45:391–7.
- [20] Park S, Lee S, Lee Y, Seo Y. CO<sub>2</sub> Capture from simulated fuel gas mixtures using semiclathrate hydrates formed by quaternary ammonium salts. Environ Sci Technol 2013;47:7571–7.
- [21] Gayet P, Dicharry C, Marion G, Graciaa A, Lachaise J, Nesterov A. Experimental determination of methane hydrate dissociation curve up to 55 MPa by using a small amount of surfactant as hydrate promoter. Chem Eng Sci 2005;60:5751–8.
- [22] Dicharry C, Duchateau C, Asbaï H, Broseta D, Torrè J-P. Carbon dioxide gas hydrate crystallization in porous silica gel particles partially saturated with a surfactant solution. Chem Eng Sci 2013;98:88–97.
- [23] Zhang JS, Lee JW. Equilibrium of hydrogen + cyclopentane and carbon dioxide + cyclopentane binary hydrates. J Chem Eng Data 2009;54:659–61.
- [24] Strobel TA, Koh CA, Sloan ED. Thermodynamic predictions of various tetrahydrofuran and hydrogen clathrate hydrates. Fluid Phase Equilib 2009;280:61–7.
- [25] Torrè J-P, Ricaurte M, Dicharry C, Broseta D. CO<sub>2</sub> enclathration in the presence of water-soluble hydrate promoters: hydrate phase equilibria and kinetic studies in quiescent conditions. Chem Eng Sci 2012;82:1–13.
- [26] Ricaurte M, Dicharry C, Broseta D, Renaud X, Torrè J-P. CO<sub>2</sub> removal from a CO<sub>2</sub>-CH<sub>4</sub> gas mixture by clathrate hydrate formation using THF and SDS as water-soluble hydrate promoters. Ind Eng Chem Res 2013;52:899–910.
- [27] Ricaurte M, Torrè J-P, Asbaï H, Broseta D, Dicharry C. Experimental data, modeling and correlation of carbon dioxide solubility in aqueous solutions containing low concentrations of clathrate hydrate promoters: application to CO<sub>2</sub>-CH<sub>4</sub> gas mixtures. Ind Eng Chem Res 2012;51:3157–69.
- [28] Lee J-W, Lu H, Moudrakovski IL, Ratcliffe CI, Ripmeester JA. Thermodynamic and molecular-scale analysis of new systems of water-soluble hydrate formers + CH<sub>4</sub>. J Phys Chem B 2010;114:13393–8.
- [29] Ohmura R, Matsuda S, Takeya S, Ebimuda T, Narita H. Phase equilibrium for structure-H hydrates formed with methane and methyl-substituted cyclic ether. Int J Thermophys 2005;26(5):1515–23.
- [30] Zhang JS, Lee S, Lee JW. Does SDS micellize under methane hydrate-forming conditions below the normal krafft point? J Colloid Interface Sci 2007; 315:313–8.
- [31] Watanabe K, Imai S, Mori YH. Surfactant effects on hydrate formation in an unstirred gas/liquid system: an experimental study using HFC-32 and sodium dodecyl sulphate. Chem Eng Sci 2005;60:4846–57.
- [32] Weiss E, Groenen-Sereno K, Savall A. Electrochemical mineralization of sodium dodecylbenzenesulfonate at boron doped diamond anodes. J Appl Electrochem 2007;37:1337–44.
- [33] Noik C, Bavière M, Defives D. Anionic surfactant precipitation in hard water. J Colloid Interface Sci 1987;115:36–45.

- [34] Miyake M, Yamada K, Oyama N. Self-assembling of guanidine-type surfactant. *Langmuir* 2008;24:8527–32.
- [35] Kim T-S, Kida T, Nakatsuji Y, Ikeda I. Preparation and properties of multiple ammonium salts quaternized by epichlorohydrin. *Langmuir* 1996;12:6304–8.
- [36] Jager MD, De Deugd RM, Peters CJ, de Swaan Arons J, Sloan ED. A model for systems with soluble hydrate formers. *Ann NY Acad Sci* 2000;912:917–23.
- [37] Jager MD, De Deugd RM, Peters CJ, de Swaan Arons J, Sloan ED. Experimental determination and modeling of structure II hydrates in mixtures of methane + water + 1,4-dioxane. *Fluid Phase Equil* 1999;165:209–23.
- [38] Torré J-P, Dicharry C, Ricaurte M, Daniel-David D, Broseta D. CO<sub>2</sub> capture by hydrate formation in quiescent conditions: in search of efficient kinetic additives. *Energy Proc* 2011;4:621–8.
- [39] Adisasmito S, Frank RJ, Sloan ED. Hydrates of carbon dioxide and methane mixtures. *J Chem Eng Data* 1991;36:68–71.
- [40] Svartaas TM, Gulbrandsen AC, Huseboe SBR, Sandved O. An experimental study on “un-normal” dissociation properties of structure II hydrates formed in presence of PVCAp at pressures in the region 30 to 175 bars – dissociation by temperature increase. In: *Proc. of 6th international conference on gas hydrates, Vancouver; 2008.*
- [41] Di Profio P, Arca S, Germani R, Savelli G. Surfactant promoting effects on clathrate hydrate formation: are micelles really involved? *Chem Eng Sci* 2005;60:4141–5.
- [42] Lo C, Zhang JS, Somasundaran P, Lu S, Couzis A, Lee JW. Adsorption of surfactants on two different hydrates. *Langmuir* 2008;24:12723–6.
- [43] Zhang JS, Lo C, Somasundaran P, Lu S, Couzis A, Lee JW. Adsorption of sodium dodecyl sulfate at THF hydrate/liquid interface. *J Phys Chem C* 2008;112:12381–5.
- [44] Zhang J, Lee JW. Enhanced kinetics of CO<sub>2</sub> hydrate formation under static conditions. *Ind Eng Chem Res* 2009;48:5934–42.
- [45] Beltran JG, Bruusgaard H, Servio P. Gas hydrate measurement techniques and phase rule considerations. *J Chem Thermodyn* 2012;44:1–4.
- [46] Lazzaroni MJ, Bush D, Jones R, Hallett JP, Liotta CL, Eckert CA. High-pressure phase equilibria of some carbon dioxide–organic–water systems. *Fluid Phase Equilib* 2004;224:143–54.
- [47] Gennaro A, Isse AA, Vianello E. Solubility and electrochemical determination of CO<sub>2</sub> in some dipolar aprotic solvents. *J Electroanal Chem* 1990;289:203–15.